THE JOURNAL OF BIOLOGICAL CHEMISTRY VOL. 286, NO. 5, pp. 3671–3680, February 4, 2011

The Ubiquitin Ligase MYCBP2 Regulates Transient Receptor Potential Vanilloid Receptor 1 (TRPV1) Internalization through Inhibition of p38 MAPK Signaling*[S]

Received for publication, June 15, 2010, and in revised form, November 22, 2010 Published, JBC Papers in Press, November 23, 2010, DOI 10.1074/jbc.M110.154765

Sabrina Holland, Ovidiu Coste, Dong Dong Zhang, Sandra C. Pierre, Gerd Geisslinger, and Klaus Scholich[1]

From the Institute of Clinical Pharmacology, Pharmazentrum Frankfurt/ZAFES, Klinikum der Goethe-Universität Frankfurt, Theodor-Stern-Kai 7, 60590 Frankfurt, Germany

The E3 ubiquitin ligase MYCBP2 negatively regulates neuronal growth, synaptogenesis, and synaptic strength. More recently it was shown that MYCBP2 is also involved in receptor and ion channel internalization. We found that mice with a MYCBP2-deficiency in peripheral sensory neurons show prolonged thermal hyperalgesia. Loss of MYCBP2 constitutively activated p38 MAPK and increased expression of several proteins involved in receptor trafficking. Surprisingly, loss of MYCBP2 inhibited internalization of transient receptor potential vanilloid receptor 1 (TRPV1) and prevented desensitization of capsaicin-induced calcium increases. Lack of desensitization, TRPV internalization and prolonged hyperalgesia were reversed by inhibition of p38 MAPK. The effects were TRPV-specific, since neither mustard oil-induced desensitization nor behavioral responses to mechanical stimuli were affected. In summary, we show here for the first time that p38 MAPK activation can inhibit activity-induced ion channel internalization and that MYCBP2 regulates internalization of TRPV1 in peripheral sensory neurons as well as duration of thermal hyperalgesia through p38 MAPK.

The E3-ubiquitin ligase MYCBP2 (Myc-binding protein 2; also known as protein associated with Myc (PAM))[2] is an unusual large protein with a predicted size of 510 kDa. MYCBP2 orthologs have been described in mouse as Phr1, in zebrafish as Esrom, in drosophila as Highwire and in *Caenorhabditis elegans* as RPM-1. While MYCBP2 mRNA is found in nearly all human tissues, its expression is exceptionally high in peripheral and central neurons (1–3). MYCBP2 has been shown to act as negative regulators of synaptic growth, synaptogenesis, and neurite growth in *C. elegans* (4), *Drosophila* (5), zebrafish (6), and mice (7, 8). In *C. elegans* and *Drosophila* MYCBP2-dependent growth inhibition is largely mediated by the p38 MAPK pathway (9, 10) whereas in mice the role of p38 MAPK in MYCBP2-regulated axonal growth is less clear. Whereas growth regulation of cortical axons by MYCBP2 does not involve p38 MAPK (8), MYCBP2-dependent axonal overgrowth of spinal cord motor neurons and sensory dorsal root ganglion (DRG) neurons was regulated by p38 MAPK-mediated alterations in microtubule stability (11).

Besides its role in the regulation of neuronal growth, also a function of MYCBP2 in neuronal transmission has been demonstrated. In *C. elegans* and drosophila loss-of-function mutations in the MYCBP2 orthologs decreased the number of synaptic vesicles at cholinergic and GABAergic synapses in a p38 MAPK-dependent manner (9) and reduced strength of synaptic transmission at neuromuscular junctions (5, 12, 13). More recently, it was shown that the MYCBP2 ortholog in *C. elegans*, RPM-1, prevents in central neurons activity-dependent internalization of AMPA receptors by inhibiting p38 MAPK signaling through ubiquitylation of MAPK kinase kinase 12 (MAPKKK12), (14). Loss of RPM-1 caused constitutive activation of p38MAPK leading to an increased internalization of the AMPA receptor ortholog GLR1.

Interestingly, in mammals down-regulation of MYCBP2 had an opposite effect on neuronal transmission. Here, down-regulation of MYCBP2 in the spinal cord of adult rats increased pain-like (nociceptive) behavior in a model for acute and inflammatory pain, suggesting an enhanced neuronal signaling (3). Consistent with the finding that MYCBP2 is a potent inhibitor of adenylyl cyclases (15–17), MYCBP2-knockdown in rat spinal cords facilitated G-protein-coupled receptor (GPCR)-induced cAMP synthesis, which plays a key role in central sensitization (3, 15).

In this study, we investigated the consequences of the loss of mammalian MYCBP2 on neuronal functions in peripheral sensory neurons. We found that MYCBP2-deficiency causes constitutive p38 MAPK activation which, surprisingly, prevented activity-induced internalization of the transient receptor potential vanilloid receptor 1 (TRPV1). This finding contrasts the role of MYCBP2 and p38 MAPK in AMPA receptor internalization in *C. elegans* (14) as well as the previously described role of p38 MAPK in promoting receptor internalization in mammalians (18–20). Thus, our findings suggest that p38 MAPK fulfills receptor-dependent versatile roles in the regulation of receptor internalization.

EXPERIMENTAL PROCEDURES

Materials—Mouse anti-calcitonin gene-related peptide (CGRP) and *Griffonia simplicifolia* isolectin B_4 (IB_4) were

* This work was supported by the DFG Grant SCHO817-3 and the LOEWE Lipid Signaling Forschungszentrum Frankfurt (LiFF).

[S] The on-line version of this article (available at http://www.jbc.org) contains supplemental Figs. S1–S3.

[1] To whom correspondence should be addressed: Institut für Klinische Pharmakologie, Klinikum der Goethe-Universität Frankfurt, Theodor-Stern-Kai 7, 60590 Frankfurt, Germany. Tel.: 49-0-69-6301-83103; Fax: 49-0-69-6301-83378; E-mail: Scholich@em.uni-frankfurt.de.

[2] The abbreviations used are: MYCBP2, Myc-binding protein 2; TRPV1, transient receptor potential vanilloid receptor 1; DRG, dorsal root ganglion.

purchased from Sigma. Antibodies against phospho-(Thr-180/Tyr-182) p38 MAPK, total p38, α-p38, γ-p38, myosin Va, and myosin VI were from Cell Signaling (Danvers, MA). The TRPV1 antibody showing the partial colocalization was from Dianova (Hamburg, Germany), the antibody showing the TrpV1-internalization was from Osenses (Flagstaff Hill, Australia). The antibody against HSP90 was from Santa Cruz Biotechnology. SB203580 was from LC Laboratories (Woburn, MA).

MYCBP2-deficient Mice—A targeting vector was constructed from a 8.7-kb PCR product from a 129/SV BAC clone and subsequently used to generate the MYCBP2-targeted allele mice (genOway, Lyon, France). In the verified fragment was a LoxP site cloned in the EcoRI site between exon 11 and 12. Then a LoxP-FRT-neo-FRT site was inserted with AvrII between exons 10 and 11. Thus, exon 11 was flanked by loxP sites (Fig. 1*A*). Exon 11 encodes 13 amino acid N-terminal of the RCC1-like domain, a highly conserved domain necessary for MYCBP2 function (6, 8, 17). Deletion of exon 11 leads to a shift in the open reading frame and results in the translation of 23 new amino acids after exon 11 before to reach a premature stop codon. As a result a deletion of the whole RHD1 domain and all C-terminally located amino acids is reached (8, 21). The construct was electroporated into ES cells and homologous recombinants containing both loxP sites were confirmed by Southern blot. ES cells were injected into 105 mouse blastocysts to generate germline chimeras. Germline chimeras were bred to C57/bl6 mice to produce heterozygotes for the floxed allele. The Neo selection cassette was removed by *in vivo* excision by crossing the mice with ubiquitously Flpe-expressing mice (genOway, Lyon, France). Then MYCBP2$^{lox/lox}$ mice were bred and crossed with the SNS-Cre line which was provided by Prof. Tegeder, Department for Clinical Pharmacology, University Hospital Frankfurt, (22) or the Nestin-Cre line B6Cg-Tg(Nes-cre)1Kln/J (The Jackson Laboratory, Bar Harbor, ME) (23) to delete the floxed exons in the germline. Deletion of exon 11 was confirmed by genomic PCR and RT-PCR (Fig. 1*B* and supplemental Fig. S1). Using genomic DNA as well as RNA as template, two PCR products representing wild type and deleted MYCBP2 sequences were observed in Cre-positive mice. Sequencing of both PCR products showed that deletion of exon 11 causes a shift in the open reading frame and results in the translation of 23 new amino acids before reaching a premature stop codon (supplemental Fig. S2). As a result, the functionally important RHD1 domain (17) and all C-terminally located amino acids including the Ring-finger domain (21), which carries the ubiquitin ligase activity, were deleted.

Genomic and RT-PCR—Genomic DNA was extracted from spinal cords and DRGs using the peqGold Tissue DNA Mini Kit (PeqLab, Erlangen, Germany). 1 μg of total DNA were used to amplify exon 11 of MYCBP2 with the primers 5′-GCAAGGGATATCTGCAGTTGGACACC and 3′-GGAACCTCGAGTAGCCATATTGGCTAGC. RNA was extracted from DRGs using RNeasy Micro Kit (Qiagen, Monheim, Germany). Total RNA was subjected to reverse transcription (RT) using M-MLV Reverse Transcriptase (Promega, Madison, WI) and a specific primer (5′-CCTTTCCCTCCTTGGTTCAT-3′). cDNA was amplified using the primers 5′-GAGACACTGGAACAGGA and 3′-CGTTCGTTTCCTCTTCTACC.

Antibody Array—The Panorama antibody microarray for cell signaling contained 726 different antibodies spotted in duplicate on nitrocellulose-coated glass from Sigma-Aldrich. Data generation was done by Microbiochips (Paris, France). Briefly, 1 mg of DRG lysates from Cre-negative or Cre-positive MYCBP2$^{lox/lox}$ mice were labeled with Cy3 and Cy5, respectively, and then hybridized to the slides according to the manufacturer's instructions. Each block of the grid contained 2 spots of Anti CY3/5 used as positive controls and for grid positioning. In several blocks, there are also 2 spots of BSA used to check for nonspecific signal. The corresponding signals were about the background level. The positive controls showed nearly saturated signal. The intensity of each spot was calculated from the median value of the pixels contained in the spot. Local background was systematically subtracted to the signal to obtain a net signal. Each antibody was spotted in duplicate on each array. To clearly identify these values, background proximity cut-off was calculated as follows: Mean (of pixels) Local Background ± 3 SD.

Behavioral Tests—In all experiments the ethics guidelines for investigations in conscious animals were obeyed and the procedures were approved by the local Ethics Committee. The investigator was unaware of the treatments or the genotypes during all behavioral experiments. *Rotarod test:* Motor coordination was assessed with a Rotarod Treadmill for mice (Ugo Basile, Comerio, Italy) at a constant rotating speed of 32 rpm. All mice had five training sessions before the day of the experiment. The fall-off latency was averaged from five tests. The cut-off time was 90 s. Hanging wire test: For the hanging wire test animals were placed in the middle of a cage wire-lid for 5 s. Then the wire-lid was inverted, hold at about 30 cm height and the fall-off latencies were recorded (24). The cut-off time was set at 90 s. Thermal thresholds were determined using the tail-flick test (25), the hot-plate test (26) and the radiant heat (Hargreaves) test (27) as described previously. For cold plate testing the mice were placed on a cold steel plate (5 + 0.5 °C) and the pain related behavior (licking flinching, rearing, jumping) was assessed during a 2 min interval. Mechanical thresholds of the plantar side of a hind paw were determined using a plantar aesthesiometer (Dynamic Plantar Aesthesiometer, Ugo Basile) or von Frey hairs. Here, a steel rod (2 mm diameter) was pushed against the paw with ascending force (0–5 g over a 10-s period, time resolution 0.1 s) until a strong and immediate withdrawal occurred. The paw withdrawal latency was taken to be the mean of at least four consecutive trials with at least 20 s in-between. Von Frey hair testing was performed as described previously (28). Formalin test: 20 μl of a 5% formaldehyde solution (formalin) was injected subcutaneously (s.c.) into the dorsal surface of one hindpaw. The time spent licking the formalin-injected paw and the number of flinches was recorded in 5 min intervals up to 45 min after formalin injection. Thermal hyperalgesia was determined following baseline measurements 4, 6, and 8 h after formalin injection.

Implantation of Lumbar Catheters—For intrathecal (i.th.) delivery of drugs, a spinal catheter was constructed by insert-

ing a slim polytetrafluoroethylene tube (OD 0.2 mm, ID 0.1 mm, length 2 cm, SUBL-60, Braintree Scientific, Braintree, USA) for 1 cm into a wider polyethylene tube (OD 0.61 mm, ID 0.28 mm, length 9 cm, neoLab, Heidelberg, Germany) and fixation of both tubes with cyanacrylate glue (Stabiloplast, Renfert, Hilzingen, Germany). A 2 cm longitudinal skin incision was made in anesthetized mice above the pelvic girdle and the muscles were bluntly dissected from the vertebrae to expose the L_4 and L_5 spinous processes. The L_5 spinous process and the intervertebral ligament were cut carefully, and a small hole was made on the dura with a 27-gauge needle. Then the slim part of the catheter was inserted 1 cm, so that the tip reached about L_1. The sign of a sudden tail or hind limb movement verified the proper localization of the catheter. Using cyanacrylate glue, the hole on the dura was covered and the catheter was fixed on the bone. After muscle suture, the catheter was tunneled under the skin through a trocar and pulled out from the dorsal neck area. Finally, the skin incision was sutured and the end of the catheter was sealed by melting. After surgery, mice were caged individually for 3 days to recover. Only mice without disturbances of neurological functions were used for behavioral experiments.

Immunohistochemistry—12-μm tissue slices and neurons from adult DRG cultures were fixed in 4% paraformaldehyde in PBS for 10 min, permeablized in 0.1% Triton X-100 for 5 min and blocked for 1 h in 3% BSA in PBS. Primary and secondary antibody incubations were done in PBS containing 1% BSA for 1 h each. The samples were washed three times with PBS prior mounting. Costaining with TrpV1 and both myosins, all produced in rabbit, were possible using the TSA Fluorescence System from Perkin Elmer (Waltham, MA). For analysis a Zeiss ApoTom fluorescence microscope (Zeiss, Germany) was used. Colocalization was evaluated using the Intensity Correlation Analysis of the software Image J 1.43m. The Pearson correlation (R_r), the Mander's colocalization coefficient (R) and split coefficients of the Mander's overlap the (M_1, M_2) were calculated. The ratio of the positive pixels in both channels was between 0.87 andf 1.02. TRPV1 internalization was assessed as described previously (16). Briefly, images for each experimental condition were taken and internalization occurrence was assessed by generating linear densitometric profiles of the cells using the ImageJ 1.60 software. Cells were judged to show internalization if the difference of TRPV1 signals of cytoplasm and plasma membrane decreased to less than double of the signal strength in the cytoplasm of unstimulated SNS-Cre-MYCBP2$^{lox/lox}$ cells.

DRG Primary Cultures—20–30 dorsal root ganglions (DRG) were prepared from adult mice and pooled in ice-cold Hanks' balanced salt solution (HBSS). Then the DRGs were transferred to Neurobasal-Medium (Invitrogen, Carlsbad, CA) containing 500 units/ml collagenase (Biochrome AG, Berlin, Germany) and 2.5 units/ml dispase II (Roche, Mannheim, Germany) and incubated at 37 °C for 2 h. The dissociated tissues were washed twice with medium containing 10% FCS and once with HBSS. Afterward the cells were incubated in 0.05% trypsin-EDTA (Invitrogen) for 10 min at 37 °C and washed again three times in medium before plating poly-L-lysine-covered coverslips in Neurobasal-Medium containing B27, glutamine, and 10% FCS. After 2 h, the medium was changed to Neurobasal Medium without FCS. The neurons were used for calcium imaging the next day.

Calcium Imaging—Calcium-imaging experiments were performed with primary dorsal root ganglion cells after 1 day in culture. Prior determination of intracellular calcium levels ($[Ca^{2+}]_i$), cells were incubated with 5 μM of Fura-2-AM (Biotrend, Cologne, Germany) in Neurobasal medium containing 0.02% Pluronic F-127 (Biotium) for 30 min. Fura-2 loaded cells were transferred to the perfusion-chamber continuously superfused with Hepes-buffered ringer-modified saline containing 145 mM NaCl, 5 mM KCl, 1 mM $MgCl_2$, 10 mM D-glucose, 1.25 mM $CaCl_2$, and 10 mM Hepes, pH 7.3, at room temperature (20–22 °C). Images were taken with an Axioscope 2 upright microscope (Zeiss, Jena, Germany) using a 10× Achroplan water immersion objective (Zeiss). The microscope was equipped with an Imago CCD camera, a polychrome IV monochromator (all TILL Photonics, Gräfelfing, Germany). Images were acquired and processed using Tillvision software. $[Ca^{2+}]_i$ was expressed as the ratio of the background-subtracted fluorescence emission at 510 nm (filter type LP 440) due to excitation at 340 nm and 380 nm using the Polychrom IV Monochromator (Till Photonics). For desensitization experiments cells were 4 times stimulated with 0.2 μM or twice with 0.5 or 1 μM Capsaicin/Ringer delivered via bath application for 10 s with a washing step of 12 or 15 min in between. Desensitization experiments using mustard oil included two stimulations for 30 s with 100 μM mustard oil with a washing step of 8 min. In all experiments included control stimulations with 50 mM KCl for 10 s were performed except when 4 capsaicin-stimulations were used. For the dose-response experiment the time of washing between the indicated stimulations were 15min. The baseline (first 3 min of each measurement) was used to calculate the increase in ratio (Δratio) for each cell.

RESULTS

Generation of Mice with MYCBP2 Deficiency in Nociceptive and Thermoreceptive Neurons—To investigate the consequences of a MYCBP2 deficiency in neurons of adult mice, we generated conditional MYCBP2-knock-out mice utilizing the Cre-Lox system to delete exon 11 as described under "Experimental Procedures." The generation of these mice was necessary, since constitutive MYCBP2 knock-out mice die at birth because of incorrect formation of neuromuscular junctions at the lung diaphragm (7, 8). Conditional MYCBP2 knock-out mice were generated by mating MYCBP2-floxed mice to mice expressing Cre-recombinase under control of the Nestin promoter (23) or to mice expressing Cre-recombinase under control of the promoter of the sodium channel $Na_v1.8$ (SNS) (22) (Fig. 1, *A* and *B*; supplemental Figs. S1 and S2). In Nestin-Cre mice Cre-recombinase expression is found in all neurons, while in SNS-Cre mice Cre-recombinase expression is restricted to nociceptive and thermoreceptive neurons of the dorsal root ganglia, trigeminal ganglia as well as a small proportion of proprioceptive neurons (22, 23). However, because Cre-positive Nestin-MYCBP2$^{lox/lox}$ mice showed a lethal phe-

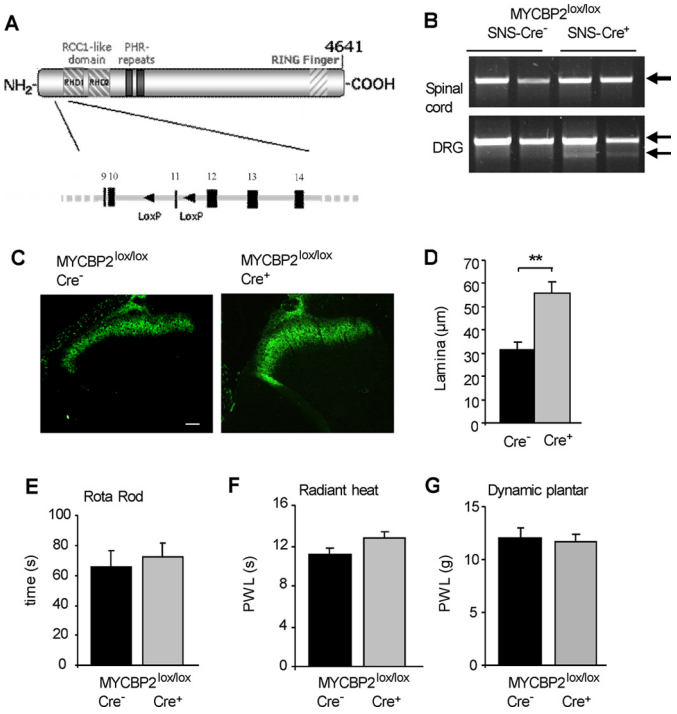

FIGURE 1. **Generation and characterization of conditional MYCBP2 knock-out mice.** *A*, scheme depicting the genomic region of the mouse *MYCBP2* gene and the inserted LOX-P sites. *B*, PCR of exon 11 using genomic DNA of spinal cords and DRGs from 2 SNS-Cre-negative and 2 SNS-Cre-positive MYCBP2$^{lox/lox}$ mice. *Arrows* indicate the wild type (*upper band*) and the deleted (*lower band*) alleles. *C*, IB4 staining of spinal cords from Cre-negative and Cre-positive MYCBP2$^{lox/lox}$ mice. The *white bar* represents 50 μm. *D*, size of lamina I and II in Cre-negative and Cre-positive MYCBP2$^{lox/lox}$ mice according to the area stained with IB4. Data are shown as average of 4–8 animals ± S.E. Two-tailed Student's *t* test; **, $p < 0.003$. *E–G*, motor coordination in Cre-negative (*black bars*) and Cre-positive MYCBP2$^{lox/lox}$ mice (*gray bars*) using the rotarod (*panel E*) test. Thermal thresholds were determined using the radiant heat test (*panel F*). Mechanical thresholds were determined using a plantar aesthesiometer (*panel G*). Data are shown as average of 7–18 animals ± S.E.

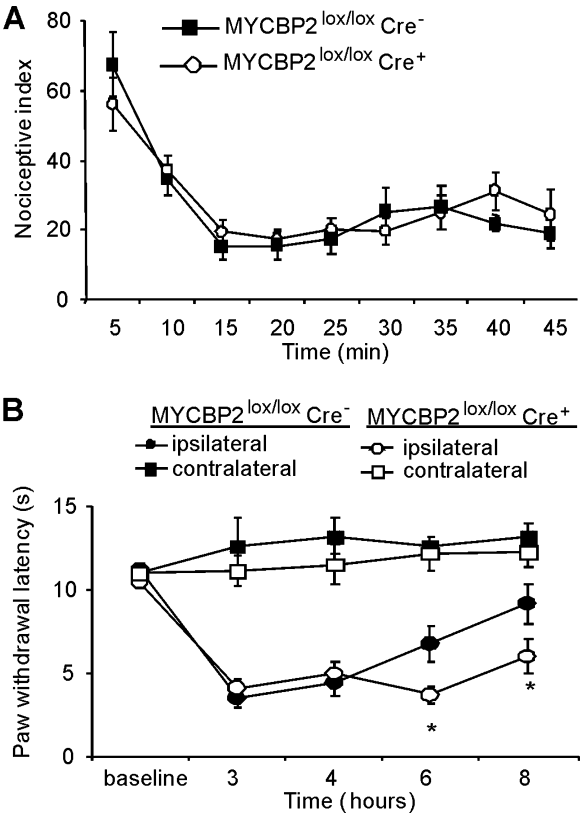

FIGURE 2. **SNS-Cre-positive MYCBP2$^{lox/lox}$ mice have prolonged thermal hyperalgesia.** *A*, formalin-evoked paw-licking behavior. Data are presented as the mean ± S.E. per 5 min intervals of 8 animals per group. *B*, time course of formalin-induced thermal hyperalgesia. Data are shown as the average of 8 animals ± S.E. Student's t-test; *, $p < 0.05$ as compared with Cre-negative mice.

notype, only the adult SNS-MYCBP2$^{lox/lox}$ mice were used in the following studies.

Because MYCBP2 negatively controls neuronal growth, we stained terminals of the primary afferents in the superficial dorsal horn of the spinal cord using the lectin *Griffonia simplicifolia* IB4 to investigate morphological consequences of the MYCBP2-deficiency. IB4 recognizes small-diameter, non-myelinated DRG neurons, which includes the sensory and thermosensitive neurons, whose central axons terminate in inner lamina II of the spinal cord (29). In accordance with the known function of MYCBP2 in restricting neuronal growth, the medial region of lamina II was enlarged in spinal cords of SNS-MYCBP2-knock-out mice (Fig. 1, *C* and *D*). However, the neuronal overgrowth had no behavioral consequences in two tests addressing the motor abilities of mice, the rotarod and the hanging wire test (Fig. 1*E* and supplemental Fig. S3*A*). Also, no differences between SNS-MYCBP2 knock-out mice and Cre-negative littermate control mice were seen in basal thermal pain thresholds as determined by the radiant heat, hot plate, and the cold plate test (Fig. 1*F* and supplemental Fig. S3*B*) or in basal mechanical thresholds as determined with a plantar aesthesiometer or von Frey hairs (Fig. 1*G* and supplemental Fig. S3*D*). Taken together, the data show that neither the overgrowth of the central terminals nor the loss of MYCBP2 causes fundamental changes in basal functions of the sensory neurons.

Regulation of TRPV1 Internalization by MYCBP2—To investigate physiological consequences of MYCBP2 deficiency in peripheral nociceptive neurons, we tested pain thresholds of SNS-MYCBP2-deficient mice in an inflammatory model. In the early phase of the formalin test, the nociceptive behavior did not differ between both animal groups (Fig. 2*A*). However, duration of the formalin-induced thermal hyperalgesia was prolonged in the MYCBP2-deficient animals (Fig. 2*B*). 6 and 8 h after formalin injection paw withdrawal latencies of SNS-MYCBP2 knock-out mice were significantly lower as compared with Cre-negative control mice (Fig. 2*B*).

Next, we studied the effect of the MYCBP2-deficiency on protein expression in DRGs, to determine the mechanistic basis for the increased duration of hyperalgesia in MYCBP2-deficient cells. Protein expression was determined by hybridizing DRG protein extracts from Cre-positive SNS-MYCBP2 knock-out mice and Cre-negative littermate control mice to an antibody microarray covering 750 proteins. 28 proteins showed a change of expression with a net log of 0.5 or more. Out of these, 11 proteins were involved in cytoskeletal-dependent processes including receptor trafficking, vesicle transport or growth regulation (Table 1). Another 10 proteins were involved in the regulation of gene expression, and 7 proteins

TABLE 1
Protein expression changes in PAM-deficient DRGs
Only proteins with log2 ratios above 0.5 or below −0.5 are shown.

Protein	Log2 (ratio Cre+/Cre-)
Cytoskeleton associated	
Cadherin	1.26
ROCK2	1.22
PKCβ1	0.92
p130^{Cas}	0.74
Tenascin	0.63
Myosin VI	0.6
Myosin Va	0.54
Reelin	0.5
GRP1	−0.53
Neurofilament 200	−0.53
MAPT	−0.58
Signaling/ubiquitylation	
SUMO1	1.14
Oaz3	1.06
Adap	0.94
Siah2	0.72
Calretinin	0.6
Caspase 4	0.5
Psen2	−0.51
Transcription	
WSTF	0.86
SP1	0.62
AP endonuclease	0.57
Y14	0.57
Tal	0.56
HDAC5	0.54
Aly	−0.54
c-Myc	−0.56
ATM	−0.67
Sin3A	−0.83

were related to general signaling events or ubiquitylation. Because MYCBP2 has recently been described to regulate receptor trafficking and the antibody array suggests changes in the trafficking machinery, we studied whether this property of MYCBP2 underlies the prolonged hyperalgesia. The antibody array suggests increased protein levels of myosin Va and myosin VI in MYCBP2-deficient DRGs, which are both known to be involved in receptor internalization and recycling (30–33). A significant up-regulation of both myosin isoforms in DRGs of SNS-MYCBP2-knock-out mice was detected in the array by two different antibodies against each protein and was confirmed by Western blot analyses (Fig. 3, *A* and *B*). To study whether or not an altered regulation of activity-dependent receptor internalization is involved in the increased duration of thermal hyperalgesia, we first studied the effect of MYCBP2 deficiency on the well characterized ion channel TRPV1, which is a receptor for noxious heat. TRPV1 is selectively activated by capsaicin, undergoes activity-induced desensitization and partially colocalized with both myosin isoforms in neuronal DRG cultures from adult Cre-negative SNS-MYCBP2 knock-out mice (Fig. 3, *C* and *D*). Notably, the colocalization frequency of TRPV1 and both myosins increased significantly after capsaicin-induced TRPV1 internalization indicating the participation of both myosins in internalization/recycling of TRPV1. The Mander's overlap coefficients for colocalization significantly increased (*t* test, $p < 0.0002$; $n = 10$) after capsaicin-induced TRPV1 internalization for Myosin Va (0.824 ± 0.0006 to 0.888 ± 0.011) and VI (0.788 ± 0.011 to 0.914 ± 0.014). Likewise, the split coefficients of the Mander's colocalization coefficients for Myosin Va (0.923 ± 0.02 to 0.987 ± 0.002) and VI (0.889 ± 0.027 to 0.996 ± 0.0007) were significantly increased $p < 0.02$ and $p < 0.001$, respectively.

To determine whether TRPV1 desensitization and/or internalization were altered in SNS-MYCBP2 knock-out mice, we determined in a first approach the desensitization of transient calcium increases in cultured adult DRG neurons in response to the TRPV1-agonist capsaicin. No significant differences in the amplitudes of capsaicin-induced intracellular calcium increases were seen between DRG neurons from MYCBP2-deficient mice and control mice using 0.1, 0.2, or 0.5 μM capsaicin (Fig. 4, *A* and *B*) showing that TRPV1 activation are unaltered in absence of MYCBP2. Next, we tested whether or not desensitization of capsaicin responses are modulated by MYCBP2. Therefore, cultured DRG neurons were stimulated consecutively with capsaicin to induce activity-dependent desensitization. Four stimulations with 0.2 μM as well as two stimulations with 0.5 μM or 1 μM capsaicin caused significant reductions in the amplitude of the capsaicin-induced calcium increase in DRG neurons from Cre-negative SNS-MYCBP2 knock-out mice (Fig. 4, *C–F*). In contrast, DRG neurons from Cre-positive SNS-MYCBP2-knock-out mice showed no significant reduction in the capsaicin-induced calcium increases in either protocol (Fig. 4, *D*, *G*, *H*).

Because the up-regulation of myosin Va and VI indicates an altered receptor trafficking in MYCBP2-deficient DRGs, we studied whether a decreased internalization of TRPV1 might be the cause for the apparent lack of desensitization. Therefore, we stimulated, as described above, peripheral sensory neurons from Cre-negative and Cre-positive SNS-MYCBP2 mice twice with 1 μM capsaicin and compared the localization of TRPV1 in stimulated and unstimulated neurons. The percentage of capsaicin-responsive cells was in both genotypes (57.1% for Cre-negative and 55.5% for Cre-positive) comparable. Interestingly, we observed that capsaicin-induced TRPV1-internalization occurred only in Cre-negative but not in Cre-positive SNS-MYCBP2 knock-out mice (Fig. 5, *A* and *B*). Thus, so far the data show that the presence of MYCBP2 is necessary for activity-induced TRPV1 internalization.

p38 MAPK Activation Prevents TRPV1 Internalization—Loss of MYCBP2 causes a constitutive p38 MAPK activation in MYCBP2-deficient sensory neurons (11). However, p38 MAPK activation has been demonstrated to promote internalization of μ-opioid- and AMPA receptors which would be in contrast to our findings (14, 18, 20, 34). Therefore, we tested in the next step whether or not p38 MAPK-activation prevents TRPV1 internalization in MYCBP2-deficient neurons. In accordance with a previous report (11), we found that phosphorylation of the α and γ isoforms of p38 MAPK on threonine 180 and tyrosine 182 were increased in DRGs from SNS-MYCBP2 knock-out mice suggesting an augmented activation (Fig. 6*A*). Then, we investigated if p38 MAPK modulates TRPV1 internalization by determining the effect of the specific p38MAPK inhibitor SB203580 on desensitization of capsaicin-induced intracellular calcium increases. Preincubation of neurons with SB203580 did not influence desensitization of capsaicin-induced calcium increases in DRG neurons from Cre-negative control mice (Fig. 6, *B* and *C*). However, preincubation with SB203580 restored the ability of the

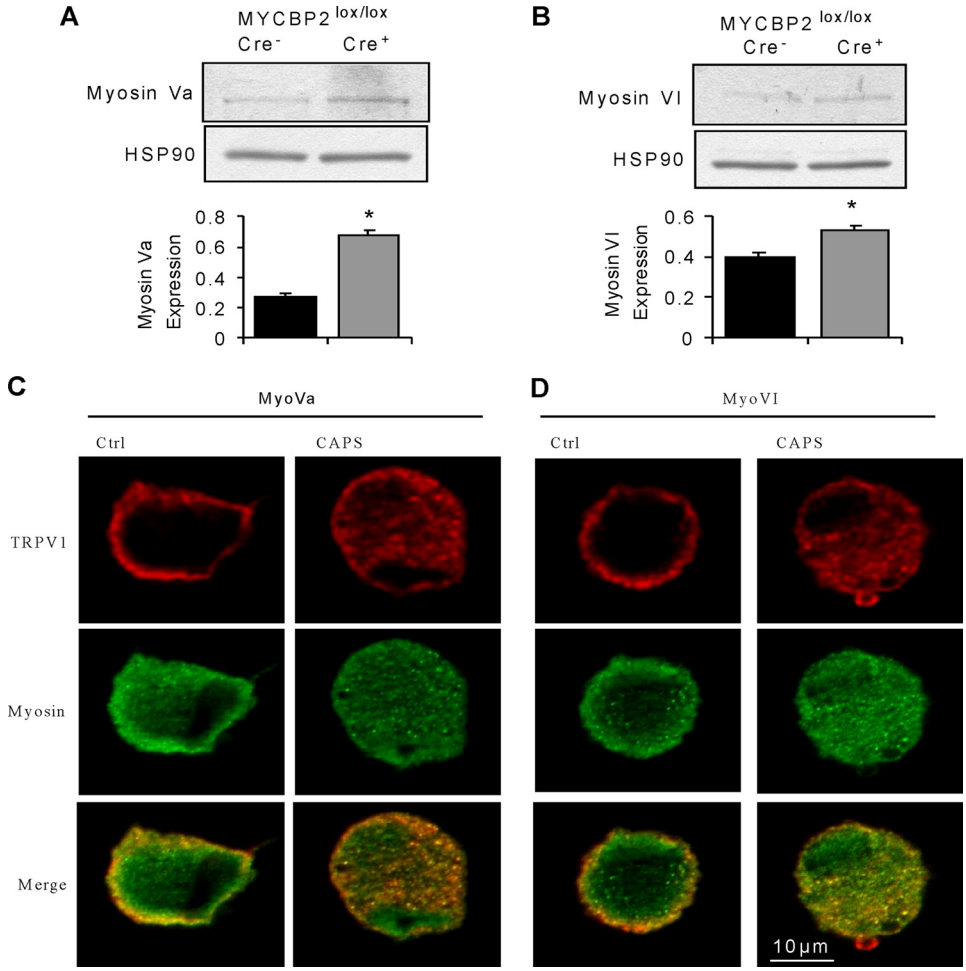

FIGURE 3. **Expression of myosin Va and myosin VI is up-regulated in DRGs from SNS-Cre-positive MYCBP2$^{lox/lox}$ mice.** *A* and *B*, Western blot analyses for myosin Va (*panel A*) and myosin VI (*panel B*) expression in DRGs from Cre-negative and Cre-positive MYCBP2$^{lox/lox}$ mice. Equal loading was confirmed using HSP90 expression. The *lower panels* show the densitometric analyses. Means are shown ± S.E. ($n = 4$). Two-tailed Student's *t* test, *, $p < 0.05$. *C–D*, immunocytochemical co-staining for myosin Va (*panel C*) or myosin VI (*panel D*) and TRPV1 of cultured DRG neurons from adult Cre-negative MYCBP2$^{lox/lox}$ mice. Neurons were stimulated twice with 1 μM capsaicin, with a washing step inbetween of 12 min. 3 min after the second stimulation, the cells were fixed in 4% PFA/PBS.

MYCBP2-deficient neurons to desensitize capsaicin-induced calcium increases (Fig. 6, *D* and *E*). Furthermore, preincubation with SB203580 restored the ability of the MYCBP2-deficient neurons to internalize TRPV1 in response to repeated capsaicin stimulations (Fig. 6, *F* and *G*). Next, SB203580 was administered intrathecally (i.th.) 4 and 6 h after formalin injection into SNS-MYCBP2 knock-out mice. While mice receiving saline showed 4 and 6 h after formalin injection significantly decreased paw withdrawal latencies, the paw withdrawal latencies of SB203580-treated animals were not significantly altered as compared with baseline (Fig. 6*H*), demonstrating the involvement of p38 MAPK in maintenance of thermal hyperalgesia in SNS-MYCBP2 knock-out mice.

Regulation of TRPV1 Internalization by MYCBP2 Is Specific—Then, we examined whether the effect of MYCBP2 on TRPV1 desensitization is specific or presents a general mechanism regulating receptor desensitization. Therefore, cultured DRG neurons were stimulated repeatedly with mustard oil, a selective activator of TRPA1, which is another member of the TRP-family of ion channels. Two consecutive stimulations with 100 μM mustard oil caused comparable reductions of the second mustard oil-induced increase of calcium concentrations in Cre-negative and Cre-positive MYCBP2-knock-out mice (Fig. 7, *A–C*). Because TRPA1 contributes significantly to the development of mechanical allodynia (35, 36), it would be expected that mechanical allodynia is not altered in Cre-positive MYCBP2-knock-out mice. Accordingly, formalin-induced mechanical allodynia was not significantly changed in SNS-MYCBP2 knock-out mice as compared with the respective control mice (Fig. 7*D*). These findings suggest that regulation of TRPV1-desensitization by MYCBP22 and p38 MAPK is a receptor-specific mechanism and not caused by a general increase of receptor trafficking.

DISCUSSION

In this report we studied the roles of MYCBP2 in thermoreceptive neurons. In accordance with its known function in synapse formation, synaptogenesis, and neurite growth (4–6, 9, 11) we found a small but significant overgrowth of the central endings of MYCBP2-deficient nociceptive and thermosensitive neurons. The limited extent of the observed overgrowth can be attributed to the fact that in these animals

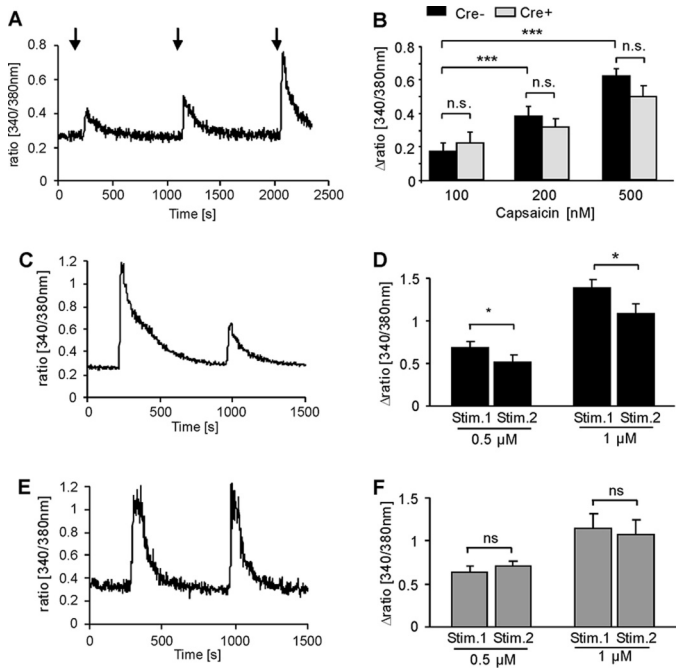

FIGURE 4. **Desensitization of capsaicin-induced calcium increases is prevented in MYCBP2-deficient DRG neurons.** *A*, neuronal cultures from adult DRGs were stimulated at the indicated times with 100, 200, and 500 nM capsaicin for 10 s. A representative experiment with neurons from Cre-negative MYCBP2$^{lox/lox}$ mice is shown. *B*, delta ratio mean of the capsaicin-induced intracellular calcium increases of neuronal DRG cultures of Cre-negative (*black bars*, $n = 42$) and Cre-positive (*gray bars*, $n = 22$) MYCBP2$^{lox/lox}$ mice. The data are given as mean ± S.E. Two-tailed Student's *t* test. ***, $p < 0.003$. *C–F*, DRG neurons from adult Cre-negative (*panels C* and *D*) or Cre-positive MYCBP2$^{lox/lox}$ (*panels E* and *F*) mice were stimulated twice with 0.5 or 1 μM capsaicin for 10 s. The mean of 17–29 cells ± S.E. is shown. Student's *t* test, *, $p < 0.05$. *Panels C* and *E* show representative tracks of stimulations with 1 μM capsaicin with neurons from Cre-negative and Cre-positive MYCBP2$^{lox/lox}$ mice, respectively.

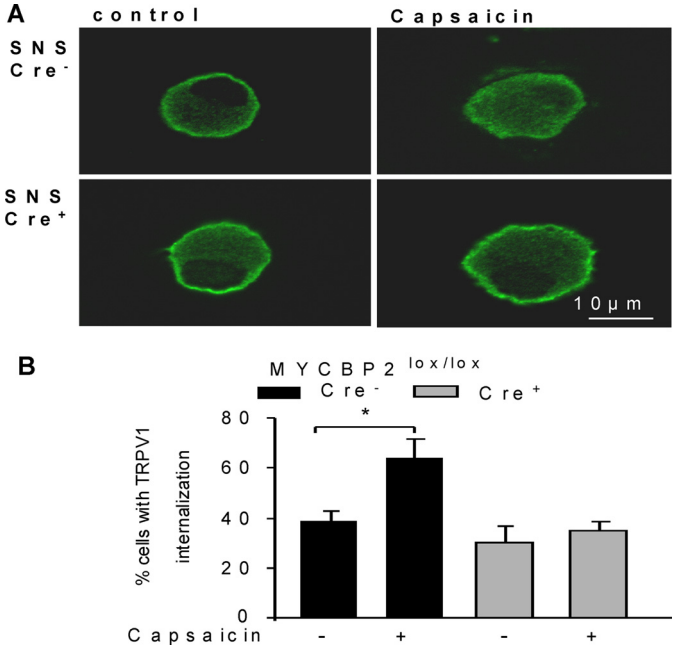

FIGURE 5. **Activity-induced TRPV1 internalization is absent in MYCBP2-deficient neurons.** *A*, representative DRG neurons from Cre-negative and Cre-positive SNS MYCBP2$^{lox/lox}$ mice were stained for TRPV1 expression. Cells were either unstimulated or stimulated twice with 1 μM capsaicin. *B*, percentage of cells with TRPV1 internalization is shown. Data are presented as average of four independent experiments. Two-tailed Student's *t* test, *, $p < 0.05$.

SNS/Cre-mediated recombination and, therefore, MYCBP2 deletion, occurs not before day 17 of the embryonal development (22). At this time formation of the synaptic connections in the spinal cord is nearly finalized and leaves only a narrow time window for additional neuronal growth in the SNS-MYCBP2 knock-out mice (37–39). The function of MYCBP2 in neurite growth regulation was also reflected by protein expression changes in DRGs from Cre-positive SNS-MYCBP2 knock-out mice in an antibody array.

In this antibody array the changes in the protein expression could be roughly separated in three groups. One group comprised proteins representing different signaling pathways. The second group included proteins involved in transcriptional regulation, which was not unexpected, because the involvement of MYCBP2 in the regulation of transcriptional and translational regulation through Myc and mTOR signaling pathways has been demonstrated previously by different groups (1, 21, 41). The largest group comprised cytoskeletal associated proteins involved in growth regulation and receptor or vesicle trafficking, such as ROCK2, myosin Va, and myosin VI (31, 33, 42). Fittingly, we found an involvement of MYCBP2 in the regulation of TRPV1 internalization.

However, it was surprising that the p38 MAPK activation prevented TRPV1 internalization in the MYCBP2-deficient neurons. Activation of p38 MAPK in MYCBP2-deficient cells is expected, because MYCBP2 targets the p38 MAPK activator MAPKKK12 through ubiquitination for proteosomal degradation. In absence of MYCBP2 MAPKKK12 accumulates and causes a constitutive activation of p38 MAPK (9, 11, 43). Also the observed prolonged thermal hyperalgesia was expected, since it was described earlier that activation of p38 MAPK in DRGs increases TRPV1 receptor protein levels at the peripheral endings of sensory neurons and prolongs thermal hyperalgesia (44–46).

Though, it was unexpected that constitutive p38 MAPK activation prevented capsaicin-induced internalization of TRPV1 receptors, because p38 MAPK activation was not known to regulate TRPV1 internalization and was previously demonstrated to promote the internalization of various receptors. Desensitization of TRP channels is mediated by different cellular pathways which are all activated by increased Ca^{2+} level. In sensory neurons and heterologous expression systems TRPV1 desensitization is due to activity-evoked activation of the calcium-dependent phosphatase PP2B, leading to dephosphorylation and desensitization of the TRPV1 channel (47, 48). It has also been reported that Ca^{2+}/calmodulin (Ca^{2+}/CaM), an ubiquitous calcium sensor, may play a role in TRPV1 Ca^{2+}-dependent desensitization by binding to the N-terminal ankyrin repeat domain (49, 50). In addition it has been shown that Ca^{2+} influx through TRPV1 activates a Ca^{2+}-sensitive phospholipase C causing depletion of phosphatidylinositol 4,5-bisphosphate (PIP_2) during desensitization, and that the recovery of the channel from desensitization requires resynthesis of PIP_2 (51–54).

Regarding the role of p38 MAPK in receptor desensitization it was shown that p38 MAPK activation was necessary

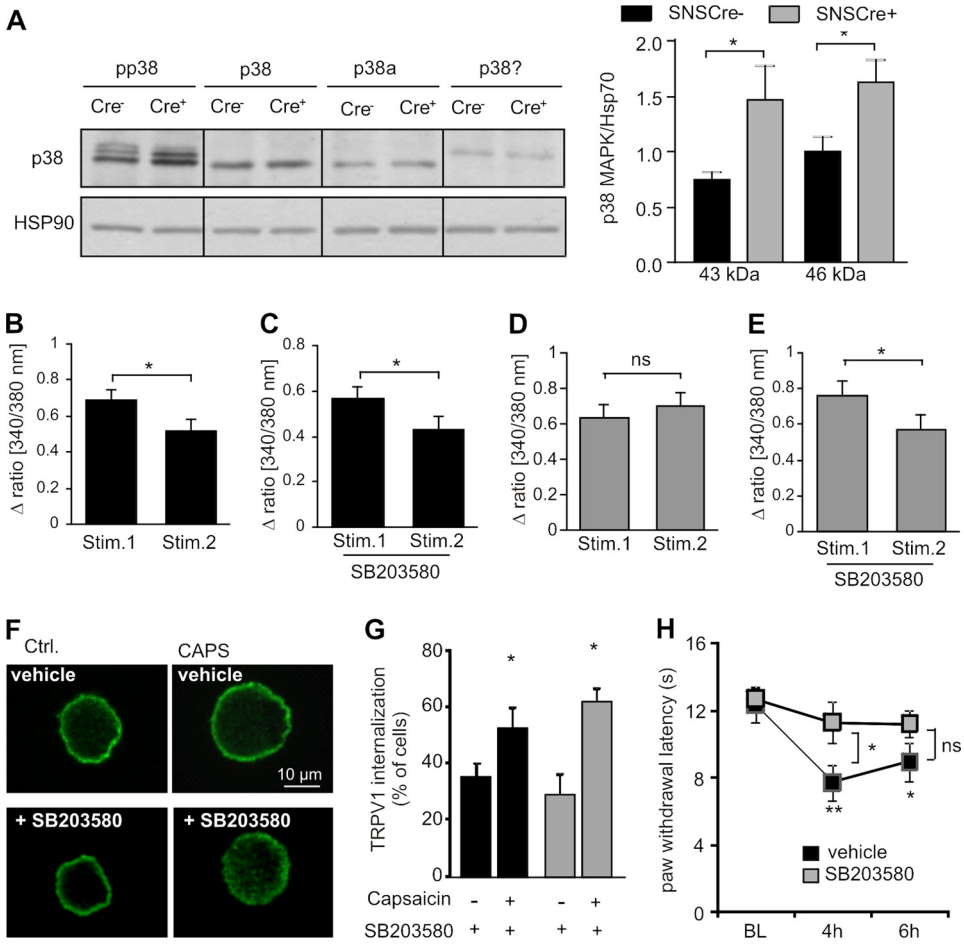

FIGURE 6. **The p38MAPK signaling pathway is activated in DRGs from Cre-positive SNS-MYCBP2$^{lox/lox}$ mice.** *A*, Western blot analysis of DRGs from naïve Cre-negative and Cre-positive MYCBP2$^{lox/lox}$ mice for phospho-p38MAPK as well as α- and γ-p38MAPK expression. The *right panel* shows the densitometric analysis of three Western blots. Student's *t* test, *, $p < 0.05$. *B–E*, delta ratio mean of capsaicin-induced maximal calcium increases in cultured DRG neurons from adult Cre-negative (*panels B* and *C*) and Cre-positive MYCBP2$^{-/-}$ mice (*panels D* and *E*) of 29–35 cells. Neurons were stimulated twice with 0.5 μM capsaicin with a recovery time of 15 min between both stimulations. In *panels C* and *E* cells were preincubated with 10 μM SB203580 for 30 min. Student's *t* test, *, $p < 0.05$. *F*, representative DRG neurons from Cre-positive SNS MYCBP2$^{lox/lox}$ mice were stained for TRPV1 expression. Cells were either unstimulated or stimulated twice with 1 μM capsaicin. Where indicated the cells were preincubated with 10 μM SB203580 for 30 min. *G*, percentage of Cre-negative and Cre-positive MYCBP2$^{lox/lox}$ cells showing TRPV1 internalization is shown. Data are presented as average of four independent experiments. Two-tailed Student's *t* test, *, $p < 0.05$. *H*, Cre-positive SNS- MYCBP2$^{lox/lox}$ mice were given intrathecally 10 μg SB203580 or saline 4 and 6 h after formalin injection (*BL*: baseline). The withdrawal latencies are shown. The data are expressed as the mean ± S.E. of 5–6 animals. Student's *t* test, *, $p < 0.05$; **, $p < 0.01$.

for μ-opioid receptor endocytosis and is even sufficient to trigger constitutive internalization of μ-opioid receptors in the absence of agonists (20). Similarly, p38 MAPK activation induced serotonine and metabotropic glutamate receptors (mGluR)-dependent long term depression by activating receptor trafficking machineries to facilitate AMPA receptor internalization (18, 34). In accordance with these reports the MYCBP2 ortholog in *C. elegans*, rpm-1, prevented in central neurons activity-dependent internalization of AMPA receptors by degrading DLK and inhibiting p38 MAPK signaling (14). In contrast to these reports, internalization of TRPV1 was absent in sensory neurons of SNS-MYCBP2 knock-out mice and was reconstituted by p38 MAPK inhibition.

Thus, our data suggest that p38 MAPK fulfills versatile roles in the modulation of activity-dependent receptor and ion-channel internalization which seem to depend on the specific receptor or ion channel. This notion that p38 MAPK fulfills different roles in receptor trafficking is further supported by the finding that regulation of receptor trafficking by p38 MAPK can occur at different stages. In this regard, it has been reported that phosphorylation of epidermal growth factor (EGF)-receptor between amino acids 1002–1022 mediates stress induced internalization (19) while EGFR phosphorylation at serine 1046 and 1047 by p38 MAPK mediates ubiquitylation and degradation of already internalized EGF receptor but not internalization itself (55, 56).

The direct ubiquitylation of TRPV1 by PAM, as described for the heme receptor Rev-erbα (57), can be ruled out, because p38 MAPK mediates the MYCBP2 effects. The mechanisms underlying the regulation of TRPV1 internalization by p38 MAPK have been partly described in other studies. One of the important downstream targets of p38 MAPK that is involved in μ-opioid receptor and AMPA receptor internalization is Rab5 (14, 18, 58), a member of the Rab family of small GTPases that function as specific regulators of vesicle transport between organelles (40, 59). After its activation Rab5 triggers endocytosis by facilitating the formation of clathrin-coated pits and sorting of membrane proteins into

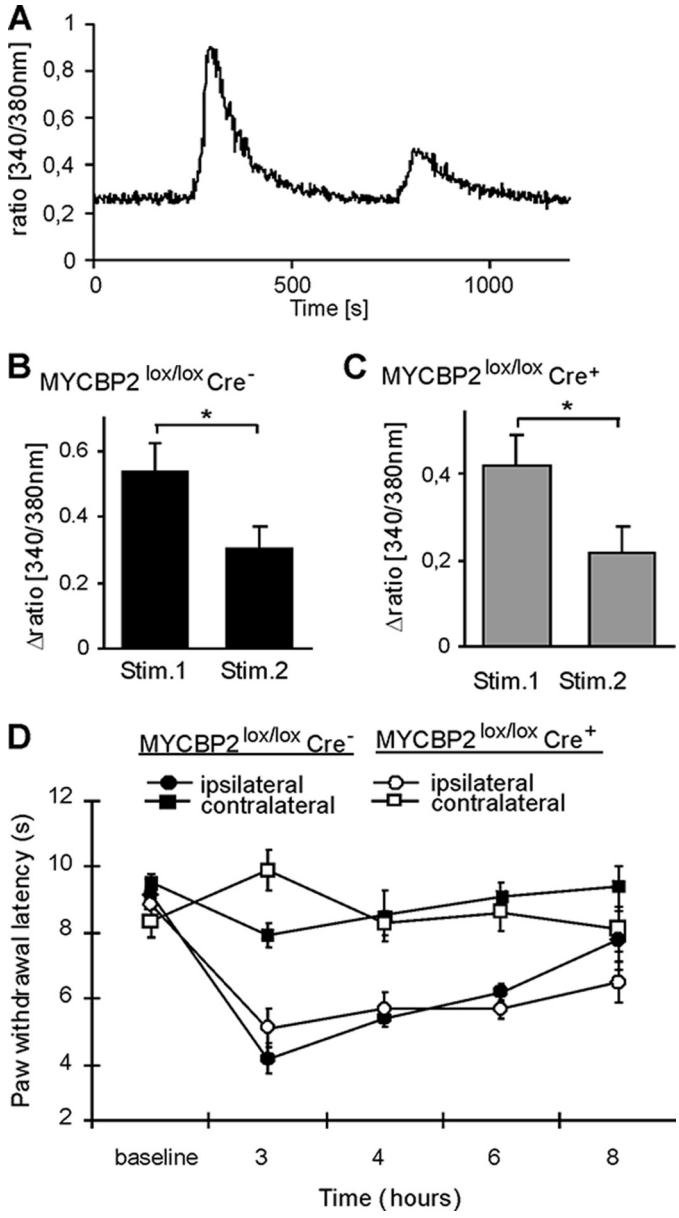

FIGURE 7. **TRPA1 desensitization is not altered in MYCBP2-deficient DRG neurons.** *A*, representative trace of mustard oil stimulation of adult DRGs from Cre-positive MYCBP2$^{lox/lox}$ mice. *B* and *C*, neuronal DRG cultures from adult MYCBP2$^{lox/lox}$ mice DRGs were stimulated twice with 100 μM mustard oil for 30 s, and maximal delta ratios (340/380 nm) were determined. Data are shown as average of 19 Cre-negative (*panel B*) and 11 Cre-positive neurons (*panel C*) ± S.E. Two-tailed Student's *t* test, *, $p < 0.05$. *C*, time course of formalin-induced mechanical allodynia. Data are shown as average of 7 animals ± S.E. *D*, time course of formalin-induced mechanical hyperalgesia. Data are shown as average of 8 animals ± S.E.

endosomes. Although Rab5-mediated endocytosis is able to explain facilitation of μ-opioid and AMPA receptor internalization by p38 MAPK, its involvement in the inhibition of TRPV1 internalization by p38 MAPK is unlikely. Taken together, we show in this report that MYCBP2 modulates TRPV1 desensitization through p38MAPK signaling which presents not only a novel model for the modulation of TRPV1-mediated signals but also expands the role of p38 MAPK in the regulation of activity-induced receptor internalization.

REFERENCES

1. Guo, Q., Xie, J., Dang, C. V., Liu, E. T., and Bishop, J. M. (1998) *Proc. Natl. Acad. Sci. U.S.A.* **95,** 9172–9177
2. Yang, H., Scholich, K., Poser, S., Storm, D. R., Patel, T. B., and Goldowitz, D. (2002) *Brain Res. Dev. Brain Res.* **136,** 35–42
3. Ehnert, C., Tegeder, I., Pierre, S., Birod, K., Nguyen, H. V., Schmidtko, A., Geisslinger, G., and Scholich, K. (2004) *J. Neurochem.* **88,** 948–957
4. Schaefer, A. M., Hadwiger, G. D., and Nonet, M. L. (2000) *Neuron* **26,** 345–356
5. Wan, H. I., DiAntonio, A., Fetter, R. D., Bergstrom, K., Strauss, R., and Goodman, C. S. (2000) *Neuron* **26,** 313–329
6. D'Souza, J., Hendricks, M., Le Guyader, S., Subburaju, S., Grunewald, B., Scholich, K., and Jesuthasan, S. (2005) *Development* **132,** 247–256
7. Burgess, R. W., Peterson, K. A., Johnson, M. J., Roix, J. J., Welsh, I. C., and O'Brien, T. P. (2004) *Mol. Cell Biol.* **24,** 1096–1105
8. Bloom A. J., M. B., Sanes J. R., and Diantonio A. (2007) *Genes & Development* **21,** 2593–2606
9. Nakata, K., Abrams, B., Grill, B., Goncharov, A., Huang, X., Chisholm, A. D., and Jin, Y. (2005) *Cell* **120,** 407–420
10. Wu, C, Daniels, R. W., and DiAntonio, A. (2007) *Neural Dev.* **2,** 16
11. Lewcock, J. W., Genoud, N., Lettieri, K., and Pfaff, S. L. (2007) *Neuron* **56,** 604–620
12. DiAntonio, A., Haghighi, A. P., Portman, S. L., Lee, J. D., Amaranto, A. M., and Goodman, C. S. (2001) *Nature* **412,** 449–452
13. Wu, C., Wairkar, Y. P., Collins, C. A., and DiAntonio, A. (2005) *J. Neurosci.* **25,** 9557–9566
14. Park, E. C., Glodowski, D. R., and Rongo, C. (2009) *PLoS One* **4,** e4284
15. Pierre, S., Eschenhagen, T., Geisslinger, G., and Scholich, K. (2009) *Nat. Rev. Drug Discov.* **8,** 321–335
16. Pierre, S. C., Häusler, J., Birod, K., Geisslinger, G., and Scholich, K. (2004) *EMBO J.* **23,** 3031–3040
17. Scholich, K., Pierre, S., and Patel, T. B. (2001) *J. Biol. Chem.* **276,** 47583–47589
18. Huang, C. C., You, J. L., Wu, M. Y., and Hsu, K. S. (2004) *J. Biol. Chem.* **279,** 12286–12292
19. Zwang, Y., and Yarden, Y. (2006) *EMBO J.* **25,** 4195–4206
20. Macé, G., Miaczynska, M., Zerial, M., and Nebreda, A. R. (2005) *EMBO J.* **24,** 3235–3246
21. Maeurer, C., Holland, S., Pierre, S., Potstada, W., and Scholich, K. (2009) *Cell Signal.* **21,** 293–300
22. Agarwal, N., Offermanns, S., and Kuner, R. (2004) *Genesis* **38,** 122–129
23. Tronche, F., Kellendonk, C., Kretz, O., Gass, P., Anlag, K., Orban, P. C., Bock, R., Klein, R., and Schütz, G. (1999) *Nat. Genet.* **23,** 99–103
24. Sango, K., McDonald, M. P., Crawley, J. N., Mack, M. L., Tifft, C. J., Skop, E., Starr, C. M., Hoffmann, A., Sandhoff, K., Suzuki, K., and Proia, R. L. (1996) *Nat. Genet.* **14,** 348–352
25. Le Bars, D., Gozariu, M., and Cadden, S. W. (2001) *Pharmacol. Rev.* **53,** 597–652
26. Tegeder, I., Del Turco, D., Schmidtko, A., Sausbier, M., Feil, R., Hofmann, F., Deller, T., Ruth, P., and Geisslinger, G. (2004) *Proc. Natl. Acad. Sci. U.S.A.* **101,** 3253–3257
27. Hargreaves, K., Dubner, R., Brown, F., Flores, C., and Joris, J. (1988) *Pain* **32,** 77–88
28. Decosterd, I., and Woolf, C. J. (2000) *Pain* **87,** 149–158
29. Silverman, J. D., and Kruger, L. (1990) *J. Neurocytol.* **19,** 789–801
30. Bridgman, P. C. (1999) *J. Cell Biol.* **146,** 1045–1060
31. Röder, I. V., Petersen, Y., Choi, K. R., Witzemann, V., Hammer, J. A., 3rd, and Rudolf, R. (2008) *PLoS One* **3,** e3871
32. Naccache, S. N., Hasson, T., and Horowitz, A. (2006) *Proc. Natl. Acad. Sci. U.S.A.* **103,** 12735–12740
33. Grant, B. D., and Donaldson, J. G. (2009) *Nat. Rev. Mol. Cell Biol.* **10,** 597–608
34. Zhong, P., Liu, W., Gu, Z., and Yan, Z. (2008) *J. Physiol.* **586,** 4465–4479
35. Bautista, D. M., Jordt, S. E., Nikai, T., Tsuruda, P. R., Read, A. J., Poblete, J., Yamoah, E. N., Basbaum, A. I., and Julius, D. (2006) *Cell* **124,** 1269–1282
36. Kwan, K. Y., Allchorne, A. J., Vollrath, M. A., Christensen, A. P., Zhang,

D. S., Woolf, C. J., and Corey, D. P. (2006) *Neuron* **50,** 277–289
37. Bennett, M. R., and Pettigrew, A. G. (1974) *J. Physiol.* **241,** 515–545
38. Dennis, M. J., Ziskind-Conhaim, L., and Harris, A. J. (1981) *Dev. Biol.* **81,** 266–279
39. Noakes, P. G., Phillips, W. D., Hanley, T. A., Sanes, J. R., and Merlie, J. P. (1993) *Dev. Biol.* **155,** 275–280
40. Sann, S., Wang, Z., Brown, H., and Jin, Y. (2009) *Trends Cell Biol.* **19,** 317–324
41. Murthy, V., Han, S., Beauchamp, R. L., Smith, N., Haddad, L. A., Ito, N., and Ramesh, V. (2004) *J. Biol. Chem.* **279,** 1351–1358
42. Roux, I., Hosie, S., Johnson, S. L., Bahloul, A., Cayet, N., Nouaille, S., Kros, C. J., Petit, C., and Safieddine, S. (2009) *Hum. Mol. Genet.* **18,** 4615–4628
43. Wu, C., Daniels, R., and DiAntonio, A. (2007) *Neural Dev.* **2,** 16
44. Mizushima, T., Obata, K., Yamanaka, H., Dai, Y., Fukuoka, T., Tokunaga, A., Mashimo, T., and Noguchi, K. (2005) *Pain* **113,** 51–60
45. Ji, R. R., Samad, T. A., Jin, S. X., Schmoll, R., and Woolf, C. J. (2002) *Neuron* **36,** 57–68
46. Bölcskei, K., Helyes, Z., Szabó, A., Sándor, K., Elekes, K., Németh, J., Almási, R., Pintér, E., Petho, G., and Szolcsányi, J. (2005) *Pain* **117,** 368–376
47. Mohapatra, D. P., and Nau, C. (2005) *J. Biol. Chem.* **280,** 13424–13432
48. Patwardhan, A. M., Jeske, N. A., Price, T. J., Gamper, N., Akopian, A. N., and Hargreaves, K. M. (2006) *Proc. Natl. Acad. Sci. U.S.A.* **103,** 11393–11398
49. Lishko, P. V., Procko, E., Jin, X., Phelps, C. B., and Gaudet, R. (2007) *Neuron* **54,** 905–918
50. Numazaki, M., Tominaga, T., Takeuchi, K., Murayama, N., Toyooka, H., and Tominaga, M. (2003) *Proc. Natl. Acad. Sci. U.S.A.* **100,** 8002–8006
51. Brauchi, S., Orta, G., Mascayano, C., Salazar, M., Raddatz, N., Urbina, H., Rosenmann, E., Gonzalez-Nilo, F., and Latorre, R. (2007) *Proc. Natl. Acad. Sci. U.S.A.* **104,** 10246–10251
52. Klein, R. M., Ufret-Vincenty, C. A., Hua, L., and Gordon, S. E. (2008) *J. Biol. Chem.* **283,** 26208–26216
53. Liu, B., Zhang, C., and Qin, F. (2005) *J. Neurosci.* **25,** 4835–4843
54. Prescott, E. D., and Julius, D. (2003) *Science* **300,** 1284–1288
55. Frey, M. R., Dise, R. S., Edelblum, K. L., and Polk, D. B. (2006) *EMBO J.* **25,** 5683–5692
56. Tong, J., Taylor, P., Peterman, S. M., Prakash, A., and Moran, M. F. (2009) *Mol. Cell Proteomics* **8,** 2131–2144
57. Yin, L., Joshi, S., Wu, N., Tong, X., and Lazar, M. A. (2010) *Proc. Natl. Acad. Sci. U.S.A.* **107,** 11614–11619
58. Cavalli, V., Vilbois, F., Corti, M., Marcote, M. J., Tamura, K., Karin, M., Arkinstall, S., and Gruenberg, J. (2001) *Mol. Cell* **7,** 421–432
59. Stenmark, H. (2009) *Nat. Rev. Mol. Cell Biol.* **10,** 513–525